Metallaheteroborane Chemistry. Part 3.† Synthesis of $[2,2-(PR_3)_2-1,2-TePtB_{10}H_{10}]$ (R_3 = Et_3, $Bu^n{}_3$, or Me_2Ph), their Characterisation by Nuclear Magnetic Resonance Spectroscopy, and the Crystal and Molecular Structure of $[2,2-(PEt_3)_2-1,2-TePtB_{10}H_{10}]$‡

George Ferguson *
Chemistry Department, University of Guelph, Guelph, Ontario, Canada N1G 2W1
John D. Kennedy and Xavier L. R. Fontaine
School of Chemistry, University of Leeds, Leeds LS2 9JT
Faridoon and Trevor R. Spalding *
Department of Chemistry, University College, Cork, Ireland

Reaction of $[Pt(PR_3)_2Cl_2]$ (R_3 = Et_3, $Bu^n{}_3$, or Me_2Ph) with the $[7-TeB_{10}H_{11}]^-$ anion in refluxing tetrahydrofuran affords the compounds $[2,2-(PR_3)_2-1,2-TePtB_{10}H_{10}]$ [R_3 = Et_3 (**1**), $Bu^n{}_3$ (**2**) or Me_2Ph (**3**)] as the major products. An *X*-ray diffraction study of (**1**) (recrystallised from CH_2Cl_2) shows the crystals to be monoclinic, space group *Cc* with four molecules in a unit cell of dimensions a = 10.387(2), b = 17.227(4), c = 14.447(3) Å, and β = 106.83(2)°. The final *R* factor was 0.020 for 2 601 observed reflections. Principal interatomic distances are Pt–Te 2.704(1), Pt–P 2.320(2) and 2.341(2), Pt–B 2.248(7)—2.295(9), Te–B 2.291(8)—2.404(8) Å. The compounds, together with the $[TeB_{10}H_{11}]^-$ precursor, have been examined by n.m.r. spectroscopy, and several interesting features are noted. Relative sign information for the various $^nJ(^{195}Pt-^1H)$ couplings to the heteroborane cluster protons is apparent from two-dimensional [$^1H-^1H$]-COSY experiments, and variable-temperature $^1H-\{^{31}P\}$ spectroscopy on compound (**3**) reveals $\Delta G^‡_{328}$ = 62 kJ mol^{-1} for the rotational metal-to-heteroborane bonding fluxionality.

A review of the literature reveals the surprising fact that, whereas twelve-vertex *closo* metallaboranes are comparatively rare,[1] related carbaborane derivatives are well established.[2,3] This is particularly noticeable for compounds which contain platinum–borane interactions. Apparently no twelve-vertex *closo*-metallaborane containing a single platinum atom is yet known (although two Pt_2B_{10} species have been characterised).[1] In platinum–carbaborane chemistry several PtC_2B_9 compounds have been prepared either by reaction of platinum(0) phosphine complexes with eleven-vertex C_2B_9 substrates,[4] or by reaction of $[Pt(cod)Cl_2]$ (cod = cyclo-octa-1,5-diene) with $[C_2B_9H_{11}]^{2-}$.[5] Similarly, the reaction of $[Pt(trans-PhCH{=}CHPh)(PEt_3)_2]$ (PhCH=CHPh = stilbene) with $[NMe_4][CB_{10}H_{11}]$ afforded a $PtCB_{10}$ product.[6] It is interesting to note in an early report that, whereas a variety of reactions could be used to prepare $[M(C_2B_9H_{11})_2]^{n-}$ complexes (n = 0—2) of nickel and palladium, similar reactions failed to produce the platinum analogues.[5] However, a later paper has reported the solid-state structure of the *commo* compound $[3,3'-Pt(1,2-C_2B_9H_{11})_2]$ which had been prepared from the reaction of 'chloroplatinic acid' in Pr^iOH with either $K[C_2B_9H_{12}]$ or $C_2B_9H_{13}$.[7]

For twelve-vertex *closo* complexes with heteroboranes other than carbaboranes as ligands, only the compounds $[Pt(PEt_3)_2(SB_{10}H_{10})]$[8] and $[2,2-(PPh_3)_2-1,2-SePtB_{10}H_{10}]$[9] have been described. The former was prepared from the reaction between $[Pt(PEt_3)_2Cl_2]$ and $[SB_{10}H_{10}]^{2-}$ and the latter was isolated from the reaction of $[Pt(PPh_3)_4]$ and $SeB_{11}H_{11}$. We now report the preparation of the first platinatelluraboranes $[2,2-(PR_3)_2-1,2-TePtB_{10}H_{10}]$ (R_3 = Et_3, $Bu^n{}_3$, or Me_2Ph) and their structural characterisation by n.m.r. spectroscopy and (for R = Et) *X*-ray diffraction techniques. We have also studied the rotation of the $Pt(PR_3)_2$ unit above the TeB_4 face to which it is bonded and have measured the free energy of activation for the process using variable-temperature n.m.r. spectroscopy (for R_3 = Me_2Ph).

Results and Discussion

The platinum(II) complexes $[Pt(PR_3)_2Cl_2]$ (R_3 = Et_3, $Bu^n{}_3$, or Me_2Ph) react with $[7-TeB_{10}H_{11}]^-$ in a 1:1 mol ratio in refluxing tetrahydrofuran (thf) to give several products. After isolation by preparative t.l.c. and recrystallisation from dichloromethane, the major product in each case showed C and H analyses consistent with the formulation $[Pt(PR_3)_2TeB_{10}H_{10}]$. The yields of the air-stable red crystalline compounds [R_3 = Et_3 (**1**), $Bu^n{}_3$ (**2**), or Me_2Ph (**3**)] were 28—49%. The addition of an equimolar quantity of NEt_3 to the reaction mixture did not appreciably affect the yields.

In order to ascertain the solid-state geometry of the platinatelluraboranes, and because no telluraboranes or their derivatives had been structurally characterised in the solid state previously, it was decided to undertake a single-crystal *X*-ray diffraction study of (**1**). Suitable crystals were grown by the slow evaporation of a solution of (**1**) in dichloromethane. Figure 1 presents a perspective view of a molecule of (**1**) and the cage atomic numbering scheme. Table 1 lists interatomic distances and selected angles. The gross cage structure is that of a distorted icosahedron with the platinum and tellurium atoms in adjacent positions. The molecule can be regarded as a derivative of $[B_{12}H_{12}]^{2-}$ with the $Pt(PEt_3)_2$ and Te units replacing Wadeian BH and BH^{2-} units respectively.[10]

The conformation of the P_2Pt group with respect to the TeB_4 face, Figure 2, is the expected one based on the analysis of the highest occupied molecular orbital (h.o.m.o.)–lowest unoccupied molecular orbital (l.u.m.o.) interactions in an analogous $SB_{10}H_{10}$ compound and is equivalent to that found in $[2,2-(PPh_3)_2-1,2-SePtB_{10}H_{10}]$.[9] The angle θ between (*a*) the

† Ref. 9 is to be regarded as Part 1; Part 2 is ref. 30*b*.
‡ *closo*-2,2-Bis(triethylphosphine)-1-tellura-2-platinadodecaborane-(10).

Supplementary data available: see Instructions for Authors, *J. Chem. Soc., Dalton Trans.*, 1988, Issue 1, pp. xvii—xx.

Table 1. Important molecular dimensions for [2,2-$(PEt_3)_2$-1,2-$TePtB_{10}H_{10}$] (**1**)

(*a*) Interatomic distances (Å)

Pt–Te	2.704(1)	C(11)–C(12)	1.506(11)	P(1)–C(1)	1.819(7)	B(6)–B(11)	1.836(10)
Pt–P(1)	2.320(2)	B(3)–B(4)	1.943(12)	P(1)–C(3)	1.832(8)	B(7)–B(8)	1.792(13)
Pt–P(2)	2.341(2)	B(3)–B(7)	1.851(12)	P(1)–C(5)	1.831(7)	B(7)–B(11)	1.798(10)
Pt–B(3)	2.295(9)	B(3)–B(8)	1.747(11)	P(2)–C(7)	1.816(7)	B(7)–B(12)	1.751(11)
Pt–B(6)	2.292(7)	B(4)–B(5)	1.908(12)	P(2)–C(9)	1.829(7)	B(8)–B(9)	1.764(11)
Pt–B(7)	2.248(7)	B(4)–B(8)	1.749(12)	P(2)–C(11)	1.840(9)	B(8)–B(12)	1.762(13)
Pt–B(11)	2.252(8)	B(4)–B(9)	1.728(12)	C(1)–C(2)	1.476(16)	B(9)–B(10)	1.799(14)
Te–B(3)	2.396(7)	B(5)–B(6)	1.948(13)	C(3)–C(4)	1.508(13)	B(9)–B(12)	1.792(14)
Te–B(4)	2.291(8)	B(5)–B(9)	1.747(12)	C(5)–C(6)	1.506(12)	B(10)–B(11)	1.802(13)
Te–B(5)	2.318(9)	B(5)–B(10)	1.741(13)	C(7)–C(8)	1.512(11)	B(10)–B(12)	1.792(11)
Te–B(6)	2.404(8)	B(6)–B(10)	1.755(11)	C(9)–C(10)	1.515(12)	B(11)–B(12)	1.782(13)

(*b*) Interatomic angles (°) around Pt, Te, P(1), P(2), and C(1), C(3), C(5), C(7), C(9), and C(11)

Te–Pt–P(1)	121.70(5)	B(3)–Te–B(4)	48.9(3)	P(2)–Pt–B(6)	86.0(2)	Pt–P(2)–C(7)	111.3(2)
Te–Pt–P(2)	104.24(5)	B(3)–Te–B(5)	83.2(3)	P(2)–Pt–B(7)	147.4(2)	Pt–P(2)–C(9)	113.6(3)
Te–Pt–B(3)	56.6(2)	B(3)–Te–B(6)	81.0(3)	P(2)–Pt–B(11)	104.1(2)	Pt–P(2)–C(11)	121.6(2)
Te–Pt–B(6)	56.8(2)	B(4)–Te–B(5)	48.9(3)	B(3)–Pt–B(6)	85.6(3)	C(7)–P(2)–C(9)	103.9(3)
Te–Pt–B(7)	94.6(2)	B(4)–Te–B(6)	82.9(3)	B(3)–Pt–B(7)	48.1(3)	C(7)–P(2)–C(11)	102.7(4)
Te–Pt–B(11)	94.7(2)	B(5)–Te–B(6)	48.7(3)	B(3)–Pt–B(11)	83.0(3)	C(9)–P(2)–C(11)	101.7(4)
P(1)–Pt–P(2)	97.70(6)	Pt–P(1)–C(1)	116.8(2)	B(6)–Pt–B(7)	82.4(3)	P(1)–C(1)–C(2)	112.9(6)
P(1)–Pt–B(3)	90.8(2)	Pt–P(1)–C(3)	113.6(3)	B(6)–Pt–B(11)	47.7(3)	P(1)–C(3)–C(4)	112.6(6)
P(1)–Pt–B(6)	176.3(2)	Pt–P(1)–C(5)	116.5(3)	B(7)–Pt–B(11)	47.1(3)	P(1)–C(5)–C(6)	117.5(6)
P(1)–Pt–B(7)	94.5(2)	C(1)–P(1)–C(3)	103.1(4)	Pt–Te–B(3)	53.1(2)	P(2)–C(7)–C(8)	115.1(5)
P(1)–Pt–B(11)	130.9(2)	C(1)–P(1)–C(5)	102.7(3)	Pt–Te–B(4)	93.1(2)	P(2)–C(9)–C(10)	115.5(5)
P(2)–Pt–B(3)	160.4(2)	C(3)–P(1)–C(5)	102.2(3)	Pt–Te–B(5)	93.0(2)	P(2)–C(11)–C(12)	116.9(6)
				Pt–Te–B(6)	52.9(2)		

(*c*) Selected interatomic angles (°) around B(3), B(4), B(5), B(6), B(7), B(9, opposite Pt), B(11), and B(12, opposite Te)

Pt–B(3)–Te	70.4(2)	B(4)–B(9)–B(5)	66.6(5)	Te–B(5)–B(4)	64.8(4)	B(7)–B(12)–B(8)	61.3(5)
Pt–B(3)–B(7)	64.6(4)	B(4)–B(9)–B(8)	60.1(5)	Te–B(5)–B(6)	67.9(4)	B(7)–B(12)–B(11)	61.2(5)
Te–B(3)–B(4)	62.7(3)	B(5)–B(9)–B(10)	58.8(5)	B(4)–B(5)–B(9)	56.2(4)	B(8)–B(12)–B(9)	59.5(5)
Te–B(3)–B(7)	118.1(4)	B(8)–B(9)–B(12)	59.4(5)	Pt–B(6)–Te	70.3(2)	B(9)–B(12)–B(10)	60.2(5)
Te–B(4)–B(3)	68.3(3)	B(10)–B(9)–B(12)	59.9(5)	Pt–B(6)–B(11)	65.0(3)	B(10)–B(12)–B(11)	60.6(5)
Te–B(4)–B(5)	66.3(3)	Pt–B(11)–B(6)	67.3(3)	Te–B(6)–B(5)	63.4(4)	Pt–B(7)–B(3)	67.3(3)
B(5)–B(4)–B(9)	57.2(5)	Pt–B(11)–B(7)	66.3(3)	Te–B(6)–B(11)	118.7(4)	Pt–B(7)–B(8)	117.2(5)
		B(6)–B(11)–B(7)	110.7(6)			Pt–B(7)–B(11)	66.5(3)
						B(3)–B(7)–B(11)	111.2(5)

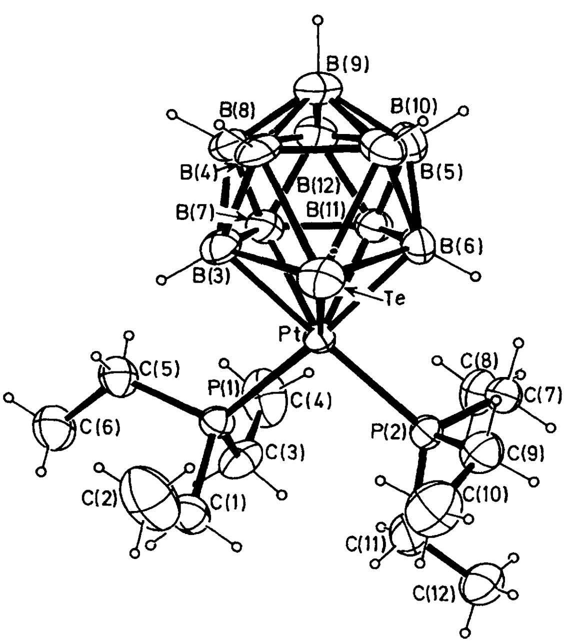

Figure 1. ORTEP plot of [2,2-$(PEt_3)_2$-1,2-$TePtB_{10}H_{10}$] (**1**) with boron cage numbering scheme

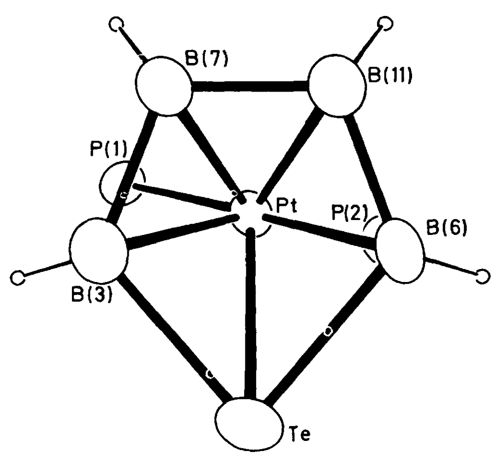

Figure 2. View of the conformation of the TeB_4 and P_2Pt units observed from the top of the TeB_4 ring

plane containing the Pt and Te atoms and the mid-point of the B(7)–B(11) vector and (*b*) that containing the P(1)P(2)Pt atoms is 102.5°, Figure 2. The corresponding angles were 100.0° in [2,2-$(PPh_3)_2$-1,2-$SePtB_{10}H_{10}$] and 104° in the isoelectronic [3,3-$(PEt_3)_2$-1,2,3-$C_2PtB_9H_{11}$].[11]

The unique Pt–Te distance of 2.704(1) Å is somewhat shorter than expected when compared to the Pt–Se distance of 2.676(1)

Å in *closo*-[2,2-$(PPh_3)_2$-1,2-$SePtB_{10}H_{10}$],[9] taking into account the difference in the published covalent radii of Te and Se (*ca.* 0.020 Å).[12] The Pt–Te distance thus implies a higher bond order in (**1**) than in the Pt–Se complex. This increased interaction can be considered to be partly due to the increased steric demands of the Te atom compared to the Se atom when placed in the B_{10} cage (see below). For comparison the Pt–S distance is 2.43 Å in *nido*-[2,2-$(PEt_3)_2$-2-H-1,2-$SPtB_9H_{10}$][13] and the covalent radius of S is 1.03 Å. In the recently reported non-cage platinum(II) complexes [Pt(1,2-$Te_2C_6H_4$)$(PPh_3)_2$][14] and [Pt{TePh(σ-$C_6H_4PPh_2$)}][Pt(SCN)$_4$]·2dmf (dmf = dimethylformamide)[15] the mean Pt–Te bond lengths were 2.589(1) and 2.586(1) Å respectively. These values must be considered representative of a two-centre two-electron bonding interaction and therefore the Pt–Te bonding in (**1**) is not of this type.

Two distinct values for the Pt–B distance are found in (**1**). The mean distance between platinum and boron atoms, B(3) and B(6), which are also bonded to Te is 2.294(9) Å whereas the value for the interaction with B(7) and B(11) which are not attached to Te is shorter at 2.250(8) Å. A similar effect was observed in [2,2-$(PPh_3)_2$-1,2-$SePtB_{10}H_{10}$] where the corresponding distances were 2.305(7) and 2.249(8) Å respectively. Both values from (**1**) can be considered typical for Pt–B interactions and fall within the range reported for numerous platinaboranes.[1] The Pt–P distances, mean 2.331(10) Å, are typical for such bonds.

The Te–B distances in the TeB_4 face attached to platinum, *i.e.* Te–B(3) and Te–B(6) are longer [mean 2.400(8) Å] than those from Te to B(4) and B(5) [mean 2.305(14) Å].

The large variations in B–B distances [from B(5)–B(6) 1.948(13) to B(4)–B(9) 1.728(12) Å] and associated B–B–B angles [for example the acute ≈60° angles in B_3 triangles which vary from B(5)–B(6)–B(10) 55.8(5) to B(5)B(10)B(6) 67.7(5)°] are typical of borane and heteroborane cage structures although the longest values are at the upper end of the 'typical' range.[1] In the present case, the B–B distances in the TeB(3)B(4)B(5)B(6) section of (**1**) are all notably longer [1.908(12)—1.948(13) Å] than the other B–B distances [1.851(12)—1.728(12) Å]. Similar effects were observed in the related *closo* Pt–Se compound.[9] These differential effects in bonding to the platinum and tellurium centres, together with the 'shorter' Pt–Te bond discussed above may suggest some diversion of bonding electron density into the Pt–Te linkage at the expense of platinum–boron and tellurium–boron bonding.

It is interesting to consider further the distortions imposed on the hypothetical regular icosahedral model compound $[B_{12}H_{12}]^{2-}$ by the introduction of the adjacent platinum and tellurium atoms. The effects may be analysed in terms of the planarity of the TeB(3)B(7)B(11)B(6) and B(4)B(8)B(12)B(10)B(5) rings, and the bonding of the B(9) atom to the above B_5 ring. In the TeB_4 ring the four boron atoms are essentially coplanar with no atom more than ±0.02 Å above or below the B_4 plane. However, the tellurium atom lies 0.147 Å below the plane containing the four B atoms, *i.e.* towards the platinum atom. In the B_5 ring the atoms lie above or below the true plane but they are not far from coplanar, the deviations being B(4) −0.011, B(8) 0.034, B(12) −0.044, B(10) 0.037, and B(5) −0.017 Å respectively. The B_5 ring is more nearly planar and the deviations are less than those reported for the equivalent part of the [3,3-$(PEt_3)_2$-1,2,3-$C_2PtB_9H_{11}$] molecule.[11] In (**1**) the B(9) atom is notably not symmetrically bonded to the B_5 ring. Two B–B distances are significantly shorter [B(9)–B(4) 1.728(12) and B(9)–B(5) 1.747(12) Å] than two others [B(9)–B(10) 1.799(14) and B(9)–B(12) 1.792(14) Å] and the fifth distance B(9)–B(8) is of an intermediate length [1.764(11) Å], Table 1. In the equivalent part of the [3,3-$(PEt_3)_2$-1,2,3-$C_2PtB_9H_{11}$] molecule the bonding was more symmetrical with all B–B distances in the range 1.767(12)—1.801(12) Å.[11] The distortions in (**1**) discussed above are presumably a function of the incorporation of the relatively large Pt and Te atoms and may be partly associated with the 'antipodal' bonding interactions which can occur through either the D^{π}, P^{σ}, or S^{σ} type orbital combinations (as classified by Stone).[16] Other possibly related antipodal effects are discussed below in relation to the n.m.r. data.

Compounds (**1**)—(**3**) were characterised by n.m.r. using single- and multiple-resonance techniques. Selected ^1H and ^{11}B

Table 3. Observed [^{11}B–^{11}B]- and [^1H–^1H]-COSY correlations for (**1**), and relaxation times $T_1(^{11}B)$ (ms) for (**1**), (**2**), and (**3**) (CD_2Cl_2 solutions, 297 K)

	(1)		$T_1(^{11}B)$ (approx.)		
Assignment	[^{11}B–^{11}B]-COSY[a,b]	[^1H–^1H]-COSY[b]	(1)	(2)	(3)
12	(8,10)s, (9)w, (7,11)w	(7,11)s, (8,10)s, (9)w	8.1	3.7	6.6
7,11	(12)w, (8,10)w	(12)s, (8,10)s, (3,6)w?	5.2	2.0	4.2
9	(12)w, (8,10)w	(12)s, (4.5)s, (8,10)s	5.3	2.5	*ca.* 4[c]
3,6		(7,11)w?, (8,10)w?	2.1	0.5	1.7
4,5	(8,10)w	(9)s, (8,10)s,	2.2	0.5	1.8
8,10	(12)s, (4,5)w, (9)w, (7,11)w	(4,5)s, (9)s, (12)s, (7,11)s, (3,6)w?	9.2	4.2	7.4

[a] Measured with {^1H(broad-band noise)} decoupling. [b] s = Stronger, w = weaker, ? = uncertain. [c] Very close ^{11}B resonances prevent more exact estimation.

Table 2. Proton and boron-11 n.m.r. data for [2,2-$(PR_3)_2$-1,2-$TePtB_{10}H_{10}$] [R_3 = Et_3 (**1**), $Bu^n{}_3$ (**2**), or Me_2Ph (**3**)] (CD_2Cl_2 solution at 297 K)

Assignment[a]	$\delta(^{11}B)$/p.p.m.[b,c]				$^1J(^{11}B-^1H)$/Hz[d]		$\delta(^1H)$/p.p.m.[e,f]		
(intensity)	(1)	(1)[g]	(2)	(3)	(1)[g]	(3)	(1)	(2)	(3)
12 (1)	+19.6	+23.1	+19.6	+19.4	153	137	+5.74	+5.67	+58.3
7,11 (2)	+9.05	+10.7[h]	+9.0	+9.1	138[h]	*ca.* 127[i]	+4.25	+4.17	+4.30
9 (1)	+7.9	+10.7[h]	+7.7	+8.4	138[h]	*ca.* 135[i]	+6.44	+6.38	+6.48
3,6 (2)	−6.8	−5.2	−6.5	−5.5	153	*ca.* 138[i]	+1.54[j]	+1.53	+1.62
4,5 (2)	−14.3	−12.8	−14.4	−14.4	162	156	+3.08	+3.04	+3.04
8,10 (2)	−21.2	−19.4	−21.3	−20.6	145	142	+1.89	+1.84	+1.97

[a] By relative intensities, incidence of satellite structure arising from $^1J(^{195}Pt-^{11}B)$, and two-dimensional [^{11}B–^{11}B]- and [^1H–^1H]-COSY experiments. [b] ±0.5 p.p.m. [c] To high frequency of BF_3·OEt_2. [d] ±8 Hz, measured from resolution-enhanced ^{11}B spectra. [e] ±0.05 p.p.m., to high frequency of $SiMe_4$. [f] ^1H Resonances related to directly bound ^{11}B resonances by selective ^1H-{^{11}B} experiments. [g] These data recorded in $CD_3C_6D_5$ solution at 373 K. [h] Accidentally coincident peaks thus only approximate values. [i] Almost coincident peaks prevent more accurate estimation. [j] Doublet splitting, *ca.* 10 Hz, possibly due to $^3J(^{31}P-^1H)$.

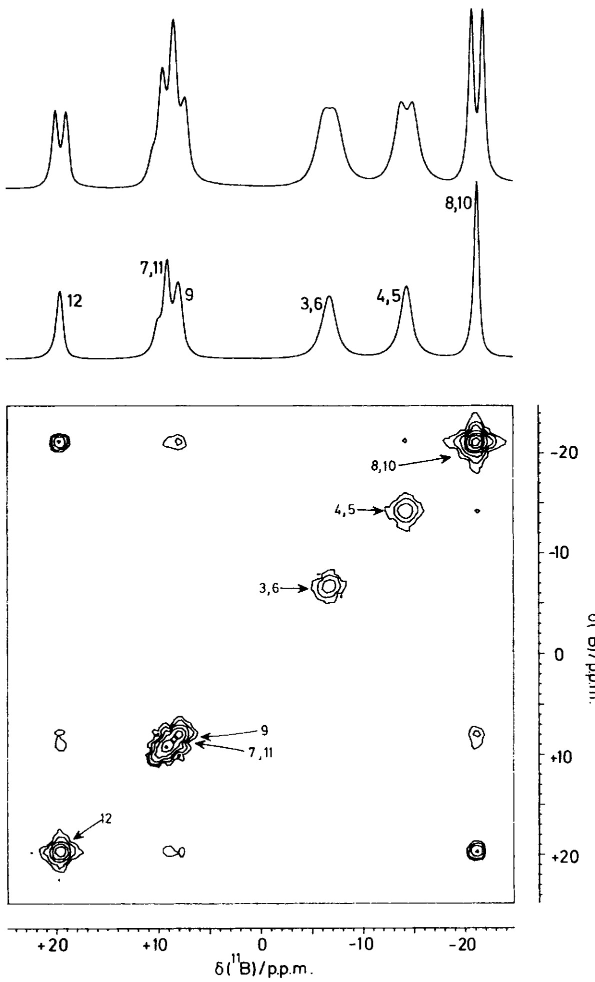

Figure 3. 128-MHz ^{11}B n.m.r. spectra for $[2,2-(PEt_3)_2-1,2-TePtB_{10}H_{10}]$ (**1**) in CD_2Cl_2 solution. The top trace is the straightforward spectrum, and the second trace was recorded with $\{^1H$(broad-band noise)$\}$ decoupling. The bottom diagram is a $[^{11}B^{11}B]$-COSY 90 plot [also with $\{^1H$(broad-band noise)$\}$ decoupling]. Note the presence of ^{195}Pt satellites to the $^{11}B(7,11)$ resonance, $^1J(^{195}Pt-^{11}B)$ *ca.* 235 Hz

chemical shift and coupling constant data for (**1**)—(**3**) are summarised in Table 2 while Table 3 contains details of $[^{11}B-^{11}B]$- and $[^1H-^1H]$-COSY data for (**1**), and longitudinal relaxation times $T_1(^{11}B)$ of the boron nuclei in (**1**)—(**3**). A symmetrised $[^{11}B-^{11}B]$-COSY plot for (**1**) is shown in Figure 3. Additional n.m.r. data relating to ^1H, ^{31}P, and ^{195}Pt nuclei are listed in the Experimental section.

Assignments to the relative atomic positions were made on the basis of $[^{11}B-^{11}B]$-[17] and $[^1H-^1H]$-COSY[18] correlations as well as chemical shift, coupling constant, relative intensity, and selective decoupling data. In general we observe similar overall shielding and intensity patterns to those of *closo*-$[2,2-(PPh_3)_2-1,2-SePtB_{10}H_{10}]$,[9] with the ten ^{11}B resonances arranged in a 1:2:1:2:2:2 sequence within a 40 p.p.m. span. This behaviour is also similar to the previously reported iron and cobalt selena- and tellura-borane compounds $[Co(\eta^5-C_5H_5)(XB_{10}H_{10})]$ and $[M(XB_{10}H_{10})_2]^{n-}$ (X = Se or Te, M = Fe or Co).[19]

A number of points arising from the n.m.r. spectroscopic results are noteworthy. We discuss principally the data from compound (**1**) although the comments apply generally. First, although there is an expected parallel between the $\delta(^{11}B)$ and $\delta(^1H)$(*exo*) values for the various BH units in the compound

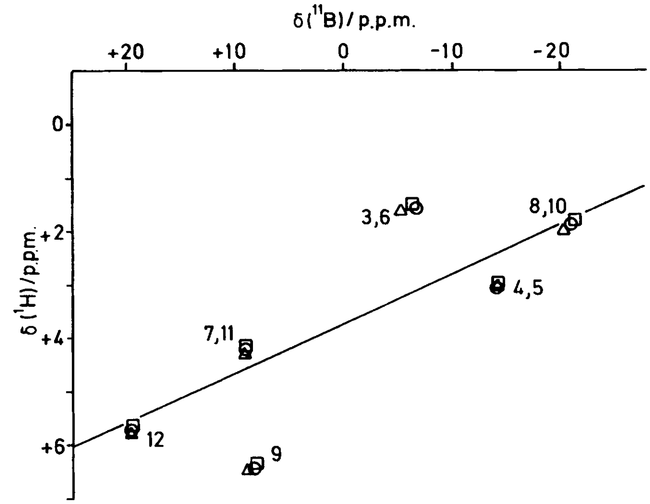

Figure 4. Plot of $\delta(^{11}B)$ *versus* $\delta(^1H)$ for the directly bound boron and hydrogen atoms of compounds (**1**) (○), (**2**) (□), and (**3**) (△). The line drawn has slope $\delta(^{11}B):\delta(^1H)$ of 11:1, and intercept $\delta(^1H)$ +3.75 p.p.m.

(Figure 4),[20] there are two significant deviations from the general trend that merit comment. The first of these concerns the $^1H(3,6)$ resonance which is some 1.5 p.p.m. above the general trend (*i.e.*, $\Delta\sigma$ +1.5 p.p.m.). This shielding increase may perhaps arise from anisotropies associated with the Pt–Te linkage which flanks this position. The second deviation is that for the $^1H(9)$ resonance which is some 2 p.p.m. below the general trend (*i.e.*, $\Delta\sigma$ −2 p.p.m.). This is the position antipodal to the platinum atom and in this context it may be noted that anomalously low proton shieldings for *exo*-terminal protons in positions antipodal to other third-row transition metals such as W, Os, and Ir have recently been noted in a variety of metallaborane systems.[21]

Another point of interest is the coupling constant information that the various experiments reveal. Coupling constants $^1J(^{195}Pt-^{11}B)$ to $^{11}B(7,11)$ and $^{11}B(3,6)$ are apparent, although the latter was only resolved with resolution enhancement techniques. That to $^{11}B(7,11)$ of 233 Hz is within normal ranges though at the lower end; that to $^{11}B(3,6)$ is therefore very low at *ca.* 125 Hz. Lower inter-*boron* coupling constants have been noted in cluster compounds in which the interboron linkage flanks a more electronegative cluster heteroatom (see later).[20,22] Presumably this also applies to the platinum–boron linkages flanking the tellurium atom, and the low values could result from a diversion of electron density towards bonds to the electronegative tellurium atom at the expense of bonds to the boron atoms adjacent to tellurium. This is not inconsistent with the observed geometrical variations discussed above.

Nearly all the protons in the platinatelluraboranes exhibit observable couplings to ^{195}Pt. The exception to this is $^1H(3,6)$ which is related to platinum *via* a ^2J path and therefore expected to have a smaller coupling constant than those linked by ^3J paths; note also that the $^1H(3,6)$ protons are bonded to the two B atoms that flank the Pt–Te linkage that induces the small $^1J(^{195}Pt-^{11}B)$ coupling referred to above. An upper limit to the magnitude of $^2J(^{195}Pt-^1H)$ based on the ^1H linewidths would be 15—20 Hz for this position. The other $^2J(^{195}Pt-^1H)$ coupling, to $^1H(7,11)$, is also small at 24 Hz and is resolvable under the solution conditions we have used only by selective $^1H-\{^{11}B\}$ spectroscopy in which the $^{11}B(7,11)$ resonance and its two ^{195}Pt satellites are each irradiated in turn.[23] These $^1H-\{^{11}B\}$ experiments also give the relative signs of

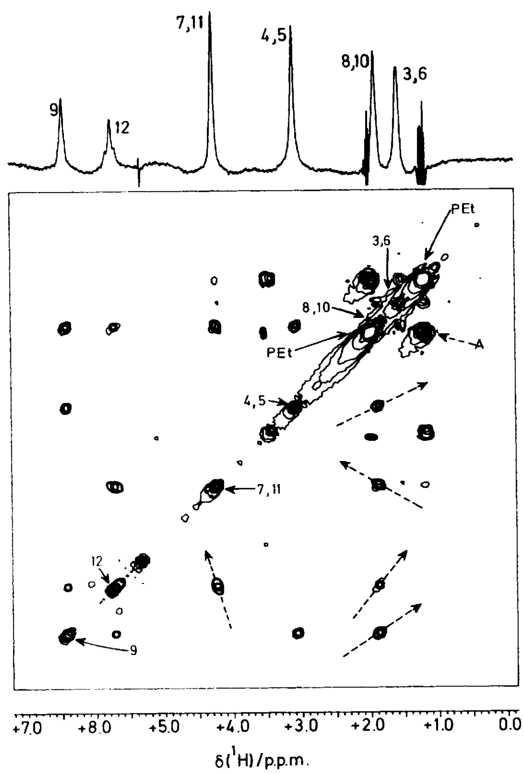

Figure 5. 400-MHz ^1H n.m.r. spectra for $[2,2\text{-}(PEt_3)_2\text{-}1,2\text{-}TePtB_{10}H_{10}]$ (**1**) in CD_2Cl_2 solution. The top trace is a $^1H\text{-}\{^{11}B$(broad-band noise)$\}$ spectrum from which an otherwise equivalent $^1H\text{-}\{^{11}B$(broad-band noise, off-resonance)$\}$ spectrum has been subtracted. The bottom diagram is a two-dimensional [^1H–^1H]-COSY 90 colour plot [also from data recorded with $\{^{11}B$(broad-band noise)$\}$ decoupling]. The tilted lozenge-shapes of some of the observed cross-correlation peaks arise from the absence or presence of correlations between the ^{195}Pt satellites of the ^1H resonances, and the slope of the tilt (dashed arrows) depends on the relative signs of the two appropriate coupling constants $^nJ(^{195}Pt\text{–}^1H)$ (see text). A tilt to the right arises from like signs, and a tilt to the left from opposite signs. The cross-correlations (A) arise between the phosphine methyl and the P–methylene protons, the direction of tilt (hatched arrow) illustrating that $^3J(^{31}P\text{–C–C–}^1H)$ and $^2J(^{31}P\text{–C–}^1H)$ are of mutually opposite sign

$^1J(^{195}Pt\text{–}^{11}B)$ and $^2J(^{195}Pt\text{–B–}^1H)$ at this position, and show that the couplings have *opposite* sign, *i.e.* $^2J(^{195}Pt\text{–}^1H)$ is negative on the reasonable assumption that $^1J(^{195}Pt\text{–}^{11}B)$ is positive.[23–25] The couplings $^3J(^{195}Pt\text{–}^1H)$ to H(8,10) and H(12) of 33 and 56 Hz respectively are within normal ranges. The lower value for $^1H(4,5)$ of *ca.* 20 Hz {apparent only from asymmetric correlations in two-dimensional [^1H–^1H]-COSY experiments discussed below (Figure 5)} for a geometrically similar coupling path is therefore of interest, although again it should be noted that this coupling path flanks the more electronegative Te position. Of interest is the incidence of a ^{195}Pt coupling to the antipodal $^1H(9)$ nucleus, formally *via* a ^4J path although there may be a substantial amount of interaction through the cluster.

The ^1H lines are broad because all the proton resonances are coupled to others, principally *via* the $^3J(^1H\text{–B–B–}^1H)$ pathways. However these couplings ensure the success of the [^1H–^1H]-COSY experiment,[18] Table 3. Interproton correlations for all the $^3J(^1H\text{–}^1H)$ coupling pairs (except one) were apparent from the two-dimensional [^1H–^1H]-COSY plot which confirms the positional assignments in Table 2 as discussed above. The one $^3J(^1H\text{–}^1H)$ correlation not observed is that between $^1H(3,6)$ and $^1H(4,5)$, and it may also be noted that some of the other correlations involving these positions are quite weak; again it is probably significant that these positions flank the more electronegative tellurium atom.

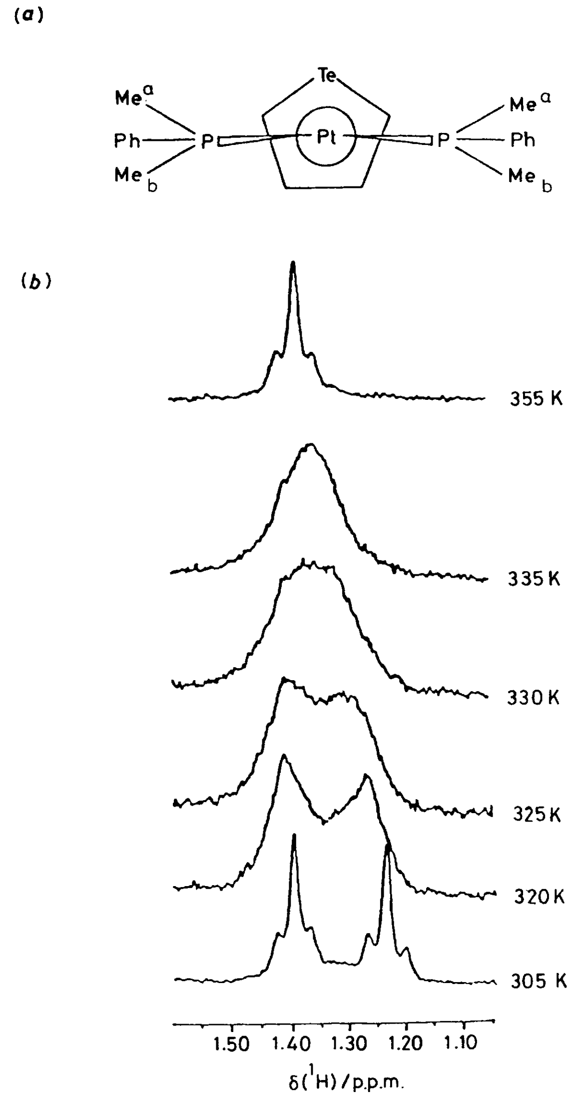

Figure 6. (*a*) An illustration of one possible conformation of the ligands about Pt in a static structure of $[2,2\text{-}(PMe_2Ph)_2\text{-}1,2\text{-}TePtB_{10}H_{10}]$ (**3**) showing two Me group environments. (*b*) 400-MHz Proton n.m.r. spectra in the Me_2PhP region of (**3**) in $CD_3C_6D_5$ solution at temperatures from 305 to 355 K

Of particular interest is the relative sign information on the couplings $^nJ(^{195}Pt\text{–}^1H)$ that is available from the [^1H–^1H]-COSY spectrum. As far as the authors are aware this kind of information has not been obtained from a [^1H–^1H]-COSY spectrum on a boron cluster compound before. Since only one ^{195}Pt satellite of a particular ^1H resonance line will be associated with one particular ^{195}Pt spin state, this satellite line will only correlate with one such satellite line of a second ^1H resonance. If the two couplings $J(^{195}Pt\text{–}^1H)$ are of the same sign, then correlations will only be observed for the low frequency–low frequency and high frequency–high frequency pairs of satellites. If of opposite sign, then only the low frequency–high frequency and high frequency–low frequency correlations will be observed. This phenomenon, together with the experimental linewidth, causes the shapes of most of the interproton cross-correlations on the contour plot to be 'lozenge-like' (Figure 5). The tilt of the 'lozenges' with respect to a vertical axis then gives the relative signs of the coupling constants $J(^{195}Pt-^{1}H)$. Interestingly the correlation for the $^{1}H(4,5)$ resonance also appears as a tilted lozenge which thereby indicates the presence of a $^{3}J(^{195}Pt-^{1}H)$ coupling that is not resolved in the $^{1}H-\{^{11}B$(broad-band noise)$\}$ spectrum. The $^{1}H-\{^{11}B\}$ results described above for the 7,11 position reasonably establish the geminal coupling $^{2}J(^{195}Pt-^{1}H)$ for this position as negative in sign and thence, *via* the two-dimensional $[^{1}H-^{1}H]$-COSY results, all the observable vicinal couplings $^{3}J(^{195}Pt-^{1}H)$ as positive. These signs are in accord with the few established patterns.[20,23–25]

The values of $\delta(^{31}P)$ and $^{1}J(^{195}Pt-^{31}P)$ are within ranges typical for bis(phosphine)platinaboranes[20] although perhaps somewhat higher than those observed for non-heteroatom-containing species.

The ^{11}B and ^{1}H chemical shift data for compounds (**2**) and (**3**) (Table 2) are very similar to those for (**1**) discussed above. For the ^{11}B spectra the principal differences reside in the successive increase in ^{11}B linewidth in the sequence $PEt_3 \leqslant PMe_2Ph < PBu^n{}_3$ (as the boron relaxation times, Table 3, increase with decrease in molecular mobility) which increasingly inhibits the resolution of coupling constants across this sequence. Interesting points include a marginal *broadening* of the central parts of the P-alkyl α-proton resonances for the three compounds upon irradiation at $\delta(^{11}B)(3,6)$, which suggests an involvement of the $^{11}B(3,6)$ spins in the $[AX_n]_2$-type spin systems ($A = {}^{31}P$, $X = {}^{1}H$). This has been noted previously in $Pt(PMe_2Ph)_2$–borane derivatives.[24]

For the dimethylphenylphosphine compound (**3**), the two methyl groups in each of the equivalent phosphine ligands are chemically distinct (even with free rotation about the platinum–phosphorus σ bonds), Figure 6(*a*). [The same will be true for the α-protons on the P–ethyl and P–butyl groups but the $\delta(^{1}H)$ differences are not so marked.] With a rotational twist of the $Pt(PMe_2Ph)_2$ unit about the pseudo-five-fold axis the chemically distinct sites are interchanged. Figure 6(*b*) shows the 400-MHz ^{1}H n.m.r. spectra for the Me_2PhP region of compound (**3**) in $CD_3C_6D_5$ recorded from 305 to 355 K. The coalescence temperature was 328 K. This gave a value of the activation energy $\Delta G^{\ddagger}_{328}$ of 62 kJ mol^{-1} for the rotational twist process of the $Pt(PMe_2Ph)_2$ unit over the TeB_4 face (allowance being made in the calculation for the differential shielding variations $d\sigma/dT$ in $CD_3C_6D_5$ of the two different Me group types). Although there are no previous $\Delta G^{\ddagger}$ values reported for the rotation of a $Pt(PR_3)_2$ unit in a *closo* compound there has been a qualitative statement that the barrier to rotation of a $Pt(PEt_3)_2$ unit over the C_2B_3 face of a *closo* seven-atom metallacarbaborane was less than that over the C_2B_3 face of a *closo* twelve-atom system.[26] A theoretical analysis of the rotational barriers in the $Pt(PH_3)_2$ analogues using extended-Hückel calculations has been attempted.[26b] It was concluded that the complex rotational process could not be taken simply as a reflection of the differences in the original displacements of the platinum atoms over the carbaborane ligand faces as had been previously suggested.[26a] Rotation of an η^4-bound $Pt(PMe_2Ph)_2$ unit with respect to a B_4 face in *nido*-$[Pt(PMe_2Ph)_2B_{10}H_{12}]$ was reported to have an activation energy of *ca.* 79 kJ mol^{-1}.[27] Several rhodium and iridium carbaborane compounds of the type $[\{MH(PR_3)_2\}C_2R_2B_9H_9]$, and related ruthenium complexes, have been studied by Hawthorne and co-workers[28] with (dynamic) ^{1}H and $^{31}P-\{^{1}H\}$ n.m.r. spectroscopy. The activation energies for the rotation of the metal-containing unit were in the range 35—$\leqslant$73 kJ mol^{-1}.

In order to complete the n.m.r. spectroscopic study of telluraborane cages presented here, we have measured n.m.r. parameters for the *nido*-$[7\text{-}TeB_{10}H_{11}]^-$ anion (Table 4, structure and numbering in Figure 7). The ^{11}B chemical shifts correspond closely to those previously reported.[19,29] They are now readily assigned in the eleven-vertex *nido* structure (**I**) on the basis of relative intensities and nearest-neighbour connectivities as established by $[^{11}B-^{11}B]$-COSY n.m.r. spectroscopy, together with the results of $^{1}H-\{^{11}B$(selective)$\}$ spectroscopy. A similar analysis of the $[7\text{-}SeB_{10}H_{11}]^-$ ion has been recently reported.[30] The resonance at $\delta(^{11}B)$ −16.8 p.p.m. is associated with the bridging proton, thus assigning this resonance to the B(9,10) position and therefore the resonance at $\delta(^{11}B)$ −18.5 p.p.m. to the B(2,3) position and those at −34.0 and −12.8 p.p.m. to the B(1) and B(5) positions respectively. All the nearest-neighbour connectivities are reflected in observed $[^{11}B-^{11}B]$-COSY correlations, although those between $^{11}B(2,3)$ and $^{11}B(8,11)$ flanking the more electronegative Te atom are very weak. This has precedent in carbaborane chemistry,[20,22,31] and also in couplings to platinum in the platinatelluraborane discussed above. The ^{1}H resonances were traced to their directly

Table 4. Measured n.m.r. parameters for Cs[*nido*-7-$TeB_{10}H_{11}$] in CD_3CN solution at 295 K

Assignment[a] (intensity)	$\delta(^{11}B)$/p.p.m.[b]	$T_1(^{11}B)$/ms (approx.)	Observed $[^{11}B-^{11}B]$-COSY correlations[c,d]	$\delta(^{1}H)$/p.p.m.[e]	$^{1}J(^{11}B-^{1}H)$/Hz	Observed $[^{1}H-^{1}H]$-COSY[d,f] correlations
4,6 (2 BH)	−5.6	54	(8,11)w, (5)m, (9,10)m, (2,3)m, (1)m	+2.91	138[g]	(8,11)m, (5)s, (9,10)w?, (2,3)w, (1)m
8,11 (2 BH)	−12.1	14	(4,6)w, (9,10)s, (2,3)vw	+2.20	165[h]	(4,6)m, (9,10)w, (2,3)m
5 (1 BH)	−12.8	46	(4,6)m, (9,10)m, (1)m	+2.79	133[i]	(4,6)s, (9,10)s, (μ)s,[k] (1)w
9,10 (2 BH)	−16.8	25	(4,6)m, (8,11)s, (5)m	+1.49	132[i]	(4,6)w?, (8,11)w, (5)s, (μ)s,[k]
(1 μ-H)[j]			(2,3)m	−3.99	44[i]	(5)m, (9,10)s,[k] (1)m[l]
2,3 (2 BH)	−18.5	14	(4,6)m, (8,11)vw, (9,10)m, (1)m	+1.77	161[g]	(4,6)w, (8,11)m, (1)m
1 (1 BH)	−34.0	74	(4,6)m, (5)m, (2,3)m	+1.26	141[g]	(4,6)m, (5)w, (μ)m,[l] (2,3)m

[a] From relative intensities, COSY correlations, and $^{1}H-\{^{11}B$(selective)$\}$ experiments that associated $^{11}B(9,10)$ with $\delta^{1}(H) = -3.99$ p.p.m. [b] ±0.5 p.p.m.; to high frequency of $BF_3 \cdot OEt_2$. [c] Measured with $\{^{1}H$(broad-band noise)$\}$ decoupling. [d] s = Stronger, w = weaker, m = intermediate. [e] ±0.05 p.p.m.; ^{1}H resonances assigned to directly bound B atoms by $^{1}H-\{^{11}B$(selective)$\}$ experiments. [f] Measured with $\{^{11}B$(broad-band noise)$\}$ decoupling. All correlations correspond to ^{3}J paths except those indicated (see footnotes *k* and *l*). [g] Measured from (resolution enhanced) ^{11}B spectrum. [h] Approximate value due to overlap with $\delta(^{11}B)$ (8,11). [i] Measured from ^{1}H spectrum. [j] Bridging position {designated (μ) in $[^{1}H-^{1}H]$-COSY column}. [k] $^{2}J(^{1}H-^{1}H)$ coupling path. [l] $^{4}J(^{1}H-^{1}H)$ coupling path.

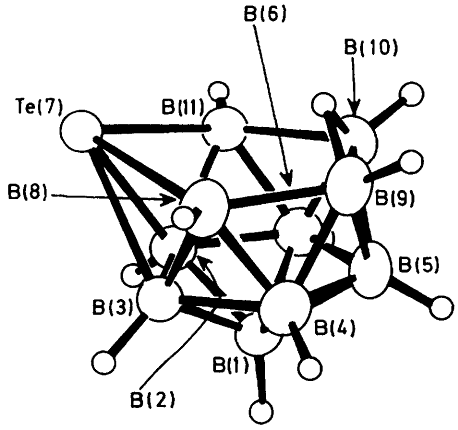

Figure 7. Proposed structure of *nido*-[7-$TeB_{10}H_{11}$]$^-$ with the atomic numbering scheme

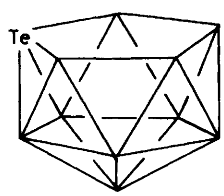

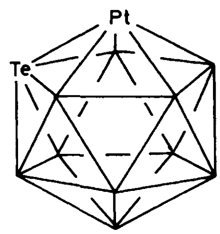

(I) **(II)**

bound boron atoms by ^1H-{^{11}B(selective)} n.m.r. spectroscopy, and they exhibited the expected general parallel between $\delta(^{11}B)$ and $\delta(^1H)$ values (Figure 8) with the bridging proton resonance some 6 p.p.m. above the general correlation. The results of [^1H–^1H]-COSY spectroscopy, carried out in the presence of {^{11}B(broad-band)} decoupling,[18] confirmed the connectivities and assignments deduced from the [^{11}B–^{11}B]-COSY work. These [^1H–^1H] correlations arise principally from the couplings $^3J(^1H$–B–B–$^1H)$, although there are also $^2J(^1H$–$^1H)$ coupling paths for the bridging protons, and there is no apparent incidence of a $^4J(^1H$–$^1H)$ coupling in this compound, between $^1H(9,10)$ (bridge) and $^1H(1)$.

It is of interest that the ^{11}B n.m.r. shielding pattern of [$TeB_{10}H_{11}$]$^-$ differs considerably from those of (**1**)—(**3**), and that there are greater similarities between the shieldings of (**1**)—(**3**) and those[29] of the *neutral* *nido*-7-chalcogenaboranes $TeB_{10}H_{12}$ and $SeB_{10}H_{12}$ (Figure 9). This suggests greater similarities in electronic structure within the neutral species, and indicates that the boron-to-platinum bonding vectors in the platinated species are more similar to those to the bridging hydrogen atoms [at H(8.9) and H(10,11)] in $TeB_{10}H_{12}$, and not similar to those to the bridging H(9,10) atom in [$TeB_{10}H_{11}$]$^-$.

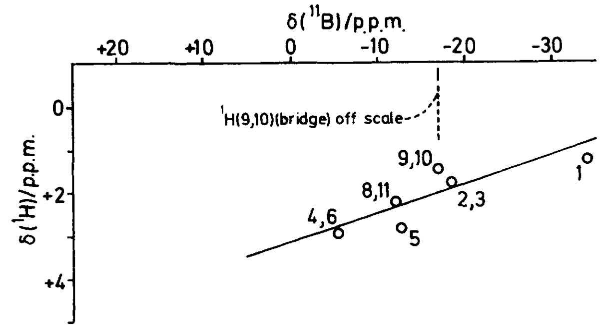

Figure 8. Plot of $\delta(^{11}B)$ *versus* $\delta(^1H)$ for directly bound boron and hydrogen atoms of the *nido*-[$TeB_{10}H_{11}$]$^-$ anion. The line drawn has slope $\delta(^{11}B)$:$\delta(^1H)$ of 15:1, with intercept $\delta(^1H)$ = *ca.* +3.13 p.p.m.

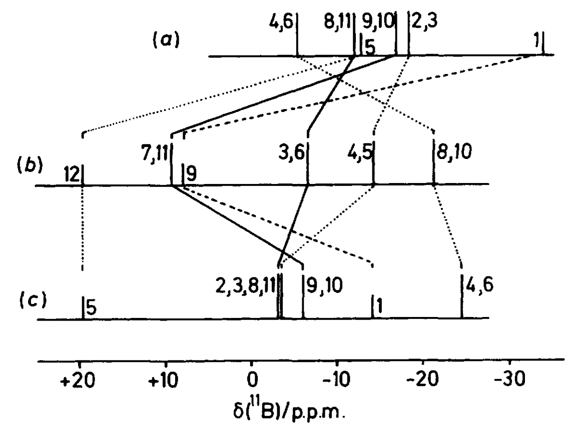

Figure 9. Stick representations of the ^{11}B chemical shifts and relative intensities of (*a*) *nido*-[7-$TeB_{10}H_{11}$]$^-$, (*b*) *closo*-[2,2-$(PEt_3)_2$-1,2-$TePtB_{10}H_{10}$] (**1**), and (*c*) *nido*-7-$TeB_{10}H_{12}$ (from ref. 29). Lines drawn link equivalent positions in two cages [(——) adjacent (α) to the Pt atom, (• • • •) metal (β) to the Pt atom, and (- - - -) antipodal to the Pt atom], and it can be seen that the shielding pattern for [$TeB_{10}H_{11}$]$^-$ is markedly different from that of compound (**1**); in fact a near-inversion in the ordering of the resonance positions has occurred whereas many basic elements of the shielding patterns for (**1**) and $TeB_{10}H_{12}$ are common, the principal differences being at the 7,11-position adjacent to the platinum atom, and at the 9-position antipodal to the platinum atom

Experimental

Both the platinum complexes [$Pt(PR_3)_2Cl_2$] (R_3 = Et_3, $Bu^n{}_3$, or Me_2Ph)[32] and the telluraborane reagents M[7-$TeB_{10}H_{11}$] (M = Cs or $NHEt_3$)[19,29] were prepared according to literature methods.

All preparative experiments were carried out under dry, oxygen-free nitrogen or methane. Subsequent manipulations were carried out in air except for recrystallisations which were done in an inert atmosphere. Analytical and preparative t.l.c. was carried out using silica gel (Merck, Kieselgel 60, PF 254) as the stationary phase and a mixture of dichloromethane–cyclohexane [(5:1) or (7:2)] as eluting solvent. Infrared spectra were recorded as KBr discs on Perkin-Elmer 457 and 682 spectrometers.

Reaction of *cis*-[$Pt(PEt_3)_2Cl_2$] *with* [$NHEt_3$][7-$TeB_{10}H_{11}$].—A solution of [$NHEt_3$][7-$TeB_{10}H_{11}$] (0.347 g, 0.99 mmol) in thf (20 cm^3) was added to a suspension of *cis*-[$Pt(PEt_3)_2Cl_2$] (0.50 g, 0.99 mmol) in thf (20 cm^3). The mixture was stirred at room temperature for 48 h and then heated at reflux for 5 min. The solution was concentrated under reduced pressure (rotary film evaporator, 25 °C). Preparative t.l.c. (CH_2Cl_2–cyclohexane, 5:1) produced three bands. The major component was extracted into CH_2Cl_2 and recrystallised as dark red *crystals* of *closo*-[2,2-$(PEt_3)_2$-1,2-$TePtB_{10}H_{10}$] (**1**) (0.237 g, 35%) (Found: C, 21.2; H, 5.8; B, 16.1. $C_{12}H_{40}B_{10}P_2PtTe$ requires C, 21.3; H, 5.9; B, 16.0%); i.r.: $\nu_{max.}$ 2 950m, 2 925s, 2 865m, 2 545vs (BH), 2 525w (BH), 2 515vs (BH), 2 500w (BH), 2 475w (BH), 1 725m,br, 1 485w, 1 448m, 1 420m, 1 415w, 1 375m, 1 370m, 1 248m, 1 070w, 1 050w, 1 035m, 1 030s, 1 010s, 1 000m, 970w, 935w, 925m, 905w, 878m, 858m, 820m, 758vs,

Table 5. Positional parameters and their estimated standard deviations

Atom	x	y	z	Atom	x	y	z
Pt	0.0 *	0.173 11(1)	0.0*	C(10)	0.294 8(10)	0.060 8(5)	0.201 1(6)
Te	−0.043 07(5)	0.172 43(3)	0.175 86(3)	C(11)	0.303 3(7)	0.077 2(5)	−0.023 4(6)
P(1)	−0.067 6(2)	0.070 76(9)	−0.107 5(1)	C(12)	0.453 6(8)	0.077 0(5)	−0.005 2(7)
P(2)	0.232 5(2)	0.155 43(9)	0.033 6(1)	B(3)	−0.210 0(8)	0.179 6(4)	0.021 8(6)
C(1)	−0.019 0(8)	−0.026 2(4)	−0.060 5(5)	B(4)	−0.234 2(8)	0.246 1(5)	0.124 1(6)
C(2)	−0.080 9(13)	−0.049 1(6)	0.015 4(7)	B(5)	−0.074 5(10)	0.305 7(5)	0.175 2(6)
C(3)	−0.001 8(7)	0.076 2(5)	−0.212 1(5)	B(6)	0.052 3(7)	0.275 7(4)	0.105 2(5)
C(4)	−0.028 8(11)	0.153 7(6)	−0.262 8(6)	B(7)	−0.180 4(8)	0.247 0(4)	−0.069 8(6)
C(5)	−0.248 7(8)	0.060 7(4)	−0.164 8(5)	B(8)	−0.291 2(8)	0.269 5(5)	0.001 2(6)
C(6)	−0.294 9(10)	−0.005 3(5)	−0.235 0(8)	B(9)	−0.217 4(9)	0.340 4(5)	0.088 6(7)
C(7)	0.313 2(6)	0.241 6(4)	0.003 9(5)	N(10)	−0.051 6(8)	0.357 9(5)	0.078 0(6)
C(8)	0.284 7(8)	0.257 6(4)	−0.103 1(6)	B(11)	−0.028 7(8)	0.302 1(5)	−0.021 5(6)
C(9)	0.318 2(7)	0.139 4(5)	0.161 8(5)	B(12)	−0.189 5(9)	0.341 8(4)	−0.028 2(6)

* The Pt x and z co-ordinates were fixed to define the origin.

720vs, 662w, and 620m cm^{-1}. Proton and ^{11}B n.m.r. spectra are summarised in Tables 2 and 3. Additional n.m.r. data: ^{195}Pt (CD_2Cl_2, 298 K) Ξ 21.378 710 MHz (δ −995 p.p.m. relative to Ξ 21.4 MHz); for B(7,11), $^1J(^{195}Pt-^{11}B)$ was (+)233 Hz; and couplings $^nJ(^{195}Pt-^1H)$ (Hz) were as follows; H(12), ^3J 56; H(7,11), ^2J −24 [sign opposite to $^1J(^{195}Pt-^{11}B)$ established by $^1H-\{^{11}B(selective)\}$ spectroscopy]; H(9), ^4J +33; H(3,6), no ^{195}Pt satellite structure apparent therefore $\leqslant$ *ca.* 15; H(4,5), ^3J $\leqslant$ +20; H(8,10), ^3J +36; $\delta(^{31}P)$ (CD_2Cl_2 solution, 298 K) +8.6 p.p.m. with $^1J(^{195}Pt-^{31}P)$ 2 903 Hz.

X-*Ray Analysis of* $[(Et_3P)_2PtTeB_{10}H_{10}]$ (**1**).—*Crystal data.* $C_{12}H_{40}B_{10}P_2PtTe$, M = 677.20, monoclinic, a = 10.387(2), b = 17.227(4), c = 14.447(3) Å, β = 106.83(2)°, U = 2 474(2) $Å^3$, Z = 4, D_c = 1.82 g cm^{-3}, $F(000)$ = 1 288, $\lambda(Mo-K_\alpha)$ = 0.710 73 Å, $\mu(Mo-K_\alpha)$ = 70.1 cm^{-1}, space group Cc or $C2/c$ from systematic absences (hkl, $h + k = 2n + 1$; $h0l$, $l = 2n + 1$). Space group Cc was chosen and confirmed by the analysis.

Structure determination. Dark red diamond-shaped crystals were grown from dichloromethane. A crystal of dimensions 0.24 × 0.27 × 0.45 mm was used for data collection. Accurate cell dimensions and crystal orientation matrix were determined on an Enraf-Nonius CAD-4 diffractometer by a least-squares treatment of the setting angles of 25 reflections in the range 11 < θ < 15°. The intensities of reflections with indices h 0 to 13, k 0 to 22, l −18 to 18 were measured with data collected in the range 2 < 2θ < 54° by the ω–2θ scan method; ω scan width (0.70 + 0.35 tanθ) using graphite-monochromatised Mo-K_α radiation. The intensities of three reflections measured every 2 h showed no evidence of crystal decay. A total of 3 036 reflections were measured of which 2 836 were unique; the 2 601 with $I > 3\sigma(I)$ were labelled observed and used in structure solution and refinement. Data were corrected for Lorentz, polarisation and absorption effects (max. and min. transmission factors 0.341 and 0.158). The space group Cc was chosen on geometrical grounds (with Z = 4, $C2/c$ would have the required symmetry of the molecule), and confirmed by analysis of the Patterson function and the successful refinement. The co-ordinates of the platinum and tellurium atoms were determined from analysis of the three-dimensional Patterson function and those of the remaining non-hydrogen atoms were found *via* the heavy-atom method. Refinement was by full-matrix least-squares calculations, initially with isotropic and then with anisotropic thermal parameters. At an intermediate stage in the refinement, difference maps showed maxima in positions consistent with the expected locations of most of the hydrogen atoms; in the final rounds of calculations the hydrogen atoms were positioned on geometrical grounds (C–H 0.95 Å, B–H 1.08 Å) and included (as riding atoms) in the structure factor calculations. The final cycle of refinement included 234 variable parameters, and a correction was refined for extinction (2.4 × 10^{-7}). R = 0.020, R' = 0.027, goodness-of-fit 1.10, $w = 1/[\sigma^2(F_o) + 0.040 (F_o)^2]$. Maximum shift/error was less than 0.005. The electron density in the final difference map was ±1.0 e $Å^{-3}$ adjacent to Pt; no chemically significant features. Scattering factors and anomalous dispersion corrections were taken from International Tables.[33] All calculations were performed on a PDP11/73 computer using the SDP-Plus suite of programs.[34] Atomic co-ordinates and details of molecular geometry are given in Tables 5 and 1 respectively. Figures 1 and 2 are views of the molecule prepared using ORTEP II.[35]

Additional material available from the Cambridge Crystallographic Data Centre comprises thermal parameters, H-atom co-ordinates, and remaining bond lengths and angles.

Reaction of cis-$[Pt(PBu^n{}_3)_2Cl_2]$ *with* $Cs[7-TeB_{10}H_{11}]$.—A solution of $Cs[7-TeB_{10}H_{11}]$ (0.142 g, 0.37 mmol) and NEt_3 (0.0377 g, 0.37 mmol) in thf (20 cm^3) was stirred at room temperature for 15 min. To this was added a solution of *cis*-$[Pt(PBu^n{}_3)_2Cl_2]$ (0.250 g, 0.37 mmol) in thf (10 cm^3). The solution was stirred at room temperature for 7 d and then heated at reflux for 24 h. After concentration of the solution under reduced pressure (rotary film evaporator, 25 °C), preparative t.l.c. (CH_2Cl_2–cyclohexane, 7:2) produced five bands. The major component was isolated after recrystallisation from CH_2Cl_2 as dark red *crystals* of *closo*-$[2,2-(PBu^n{}_3)_2-1,2-TePtB_{10}H_{10}]$ (**2**) (0.88 g, 28%) (Found: C, 33.8; H, 7.6. $C_{24}H_{64}B_{10}PtTe$ requires C, 34.1; H, 7.6%); i.r.: $\nu_{max.}$ 2 955s, 2 925s, 2 870m, 2 550s (BH), 2 500s (BH), 2 482w (BH), 1 460m, 1 420m, 1 380m, 1 345w, 1 295w, 1 270vw, 1 230w, 1 210m, 1 190w, 1 090m, 1 050w, 1 012m, 1 002m, 968, 935w, 915m, 902m, 770w, 721m, 460m, 400m, and 390w cm^{-1}. Proton and ^{11}B n.m.r. spectra are summarised in Tables 2 and 3. Additional n.m.r. data (2% in CD_2Cl_2, 297 K): $\delta(^1H)$ (P–butyl) centred at +1.91, +1.55, +1.45 and (1:2:1 triplet at 400 MHz) +0.97 p.p.m.; $^nJ(^{195}Pt-^1H)$ couplings as follows: H(7,11), ^2J *ca.* −15 Hz; and H(8,10), ^3J *ca.* 25 Hz; $^1J[^{195}Pt-^{11}B(7,11)]$ was *ca.* 240 Hz.

Reaction of cis-$[Pt(PMe_2Ph)_2Cl_2]$ *with* $Cs[7-TeB_{10}H_{11}]$.—To a solution of *cis*-$[Pt(PMe_2Ph)_2Cl_2]$ (0.182 g, 0.34 mmol) in thf (35 cm^3) was added $Cs[7-TeB_{10}H_{11}]$ (0.127 g, 0.34 mmol). The solution was stirred at room temperature for 24 h and then heated at reflux for 24 h. After concentration under reduced pressure (rotary film evaporator, 25 °C) the solution was subjected to preparative t.l.c. (CH_2Cl_2–cyclohexane, 7:2) and gave three bands. The major band was extracted with CH_2Cl_2. On recrystallisation, dark red *crystals* of *closo*-$[2,2-(PMe_2Ph)_2$-

Table 6. Experimental details for the two-dimensional n.m.r. experiments on compound (1)

	[^{11}B–^{11}B]-COSY	[^{1}H–^{1}H]-COSY
Data size (t_2, t_1)/words	256, 64	512, 128
Transform size (F_2, F_1)/words	512, 256	512, 256
t_2 Sweepwidth (= 2 × t_1 sweepwidth)/Hz	6 410.3	2 958.6
Digital resolution (F_2, F_1)/Hz per point	25, 25	11.6, 11.6
Recycling time/s	0.07	1.1
Mixing pulse/°	45	45
Window	sine-bell squared (unshifted)*	sine-bell squared (unshifted)*
Other details	continuous {^{1}H(broad-band noise)} decoupling	gated {^{11}B(broad-band noise)} decoupling

* *i.e.* Centred on the centre point of the acquired free induction decay data array (line 2) prior to zero filling to give the transform size (line 3).

1,2-TePtB$_{10}$H$_{10}$] (**3**) (0.118 g, 49%) were isolated (Found: C, 26.2; H, 4.4. $C_{16}H_{32}B_{10}P_2PtTe$ requires C, 26.8; H, 4.5%); i.r.: $\nu_{max.}$ 3 038w, 2 990w, 2 900w, 2 540vs (BH), 2 525vs (BH), 2 495vs (BH), 2 472w (BH), 1 580w, 1 562w, 1 482m, 1 470m, 1 430s, 1 420m, 1 410m, 1 315w, 1 308w, 1 292m, 1 280s, 1 268vw, 1 190w, 1 175w, 1 155w, 1 095s, 1 068w, 1 008s, 1 000w, 942s, 912vs, 905vw, 872w, 862w, 840m, 832vw, 818w, 765w, 745s, 738s, 712s, 690s, and 680m cm^{-1}. Proton and ^{11}B n.m.r. spectra are summarised in Tables 2 and 3. Additional data were as follows (CD_2Cl_2, 297 K): Ξ (^{195}Pt) 21.381 190 MHz (δ −879 p.p.m. relative to Ξ 21.4 MHz) and couplings ^{n}J(^{195}Pt–^{1}H) (Hz) were as follows: H(12), ^{3}J *ca.* 55; H(7,11), ^{2}J *ca.* −15; H(9), ^{4}J *ca.* 25; H(8,10), ^{3}J *ca.* 25; δ(^{31}P) = −14.5 p.p.m.; ^{1}J(^{195}Pt–^{31}P) 2 979 ± 6 Hz; δ(^{1}H) (P–methyl) +1.86 [N = (^{2}J + ^{4}J) (^{31}P–^{1}H) = 10 Hz; ^{3}J(^{195}Pt–^{1}H) 23 Hz] and +1.61 [N = 9.5 Hz; ^{3}J(^{195}Pt–^{1}H) 27.5 Hz]; δ(^{1}H) (P–aromatic protons) + 7.41—7.43 and +7.56—7.62 p.p.m.; selective ^{1}H-{^{11}B} using ν[^{11}B(3,6)] broadens P–methyl resonances: ^{1}J[^{195}Pt–^{11}B(7,11)] was *ca.* +240 Hz.

Nuclear Magnetic Resonance Spectroscopy.—N.m.r. spectroscopy was performed at 9.4 T using commercially available instrumentation. The techniques of ^{1}H-{^{11}B},[23,24,36–38] ^{1}H-{^{31}P},[39] [^{11}B–^{11}B]-COSY,[17,38,40,41] and [^{1}H–^{1}H]-COSY [18,38,40] n.m.r. spectroscopy as used in this work were essentially as described elsewhere.[17,18,23,24,36–41] In the ^{1}H-{^{11}B} experiments use was made of the technique[24,42] in which a ^{1}H-{^{11}B(off-resonance)} spectrum was subtracted from a ^{1}H-{^{11}B(on-resonance)} spectrum in order to remove proton resonances not coupled to the ^{11}B nucleus of interest. In the [^{11}B–^{11}B]-COSY and [^{1}H–^{1}H]-COSY experiments {^{1}H-(broad-band noise)} and {^{11}B(broad-band noise)} decoupling respectively were applied continuously, typical experimental parameters for the COSY work being summarised in Table 6. Other n.m.r. spectroscopy was straightforward, relaxation times T_1(^{11}B) being measured by the π-delay–π/2–acquire inversion–recovery method, and chemical shifts δ being quoted positive to high frequency (low field) of Ξ 100 for ^{1}H, Ξ 40.480 730 (nominally 85% H_3PO_4) for ^{31}P, Ξ 32.083 971 (nominally BF_3·OEt_2 in $CDCl_3$ for ^{11}B),[20] and Ξ 21.4 MHz[43] for ^{195}Pt (Ξ being defined as in ref. 44). For the location of the ^{195}Pt resonances, a succession of ^{1}H-{^{195}Pt(high power, selective)} experiments using the P–alkyl ^{1}H signals were first of all rapidly carried out in order to locate the approximate resonance position before acquisition of the final data by direct ^{195}Pt-{^{1}H(broad-band noise)} spectroscopy.

Acknowledgements

A generous loan of platinum salts from Johnson Matthey plc is gratefully acknowledged. G. F. would like to thank the N.S.E.R.C. Canada for Grants in Aid of Research. X. L. R. F. and J. D. K. would like to thank the S.E.R.C. for facilities and Professor N. N. Greenwood for his interest in this work. Faridoon would like to thank the Department of Education of the Republic of Ireland for a Senior Studentship.

References

1 J. D. Kennedy, *Prog. Inorg. Chem.*, 1986, **34**, 211.
2 M. P. Garcia, M. Green, F. G. A. Stone, R. G. Somerville, A. J. Welch, C. E. Briant, D. N. Cox, and D. M. P. Mingos, *J. Chem. Soc., Dalton Trans.*, 1985, 2343 and refs. therein.
3 R. E. King, D. C. Busby, and M. F. Hawthorne, *J. Organomet. Chem.*, 1985, **279**, 103 and refs. therein.
4 M. Green, J. L. Spencer, F. G. A. Stone, and A. J. Welch, *J. Chem. Soc., Dalton Trans.*, 1975, 179.
5 L. F. Warren and M. F. Hawthorne, *J. Am. Chem. Soc.*, 1970, **92**, 1157.
6 W. E. Carroll, M. Green, F. G. A. Stone, and A. J. Welch, *J. Chem. Soc., Dalton Trans.*, 1975, 2263.
7 E. A. Chernyshev, L. K. Knyazeva, Z. V. Belyakova, A. V. Kisin, N. I. Kirillova, A. I. Gusev, and N. V. Alekseev, *Zh. Obshch. Khim.*, 1983, **53**, 1289.
8 W. R. Hertler, F. Klanberg, and E. L. Muetterties, *Inorg. Chem.*, 1967, **6**, 1696.
9 G. Ferguson, M. Parvez, J. A. MacCurtain, O. Ni Dhubhghaill, T. R. Spalding, and D. Reed, *J. Chem. Soc., Dalton Trans.*, 1987, 699.
10 K. Wade, *Adv. Inorg. Chem. Radiochem.*, 1976, **18**, 1.
11 D. M. P. Mingos, M. I. Forsyth, and A. J. Welch, *J. Chem. Soc., Dalton Trans.*, 1978, 1363.
12 See, for example, N. N. Greenwood and A. Earnshaw, in 'The Chemistry of the Elements,' Pergamon Press, Oxford, 1984, ch. 6.
13 A. R. Kane, L. J. Guggenberger, and E. L. Muetterties, *J. Am. Chem. Soc.*, 1970, **92**, 2571.
14 D. M. Giolando, T. B. Rauchfuss, and A. L. Rheingold, *Inorg. Chem.*, 1987, **26**, 1636.
15 H. J. Gysling and H. R. Luss, *Organometallics*, 1984, **3**, 596.
16 A. J. Stone, *Inorg. Chem.*, 1981, **20**, 563.
17 T. L. Venable, W. C. Hutton, and R. N. Grimes, *J. Am. Chem. Soc.*, 1984, **106**, 29.
18 X. L. R. Fontaine and J. D. Kennedy, *J. Chem. Soc., Chem. Commun.*, 1986, 779.
19 J. L. Little, G. D. Friesen, and L. J. Todd, *Inorg. Chem.*, 1977, **16**, 869.
20 See, for example, J. D. Kennedy, in 'Boron,' ch. 8, in 'Multinuclear NMR,' ed. J. Mason, Plenum, London and New York, 1987, pp. 221—258 and refs. therein.
21 See, for example, I. Macpherson, Ph.D. Thesis, University of Leeds, 1987; I. Macpherson, personal communication, 1987.
22 R. J. Astheimer and L. G. Sneddon, *Inorg. Chem.*, 1983, **22**, 1928 and refs. therein.
23 J. D. Kennedy and B. Wrackmeyer, *J. Magn. Reson.*, 1980, **38**, 529.
24 S. K. Boocock, N. N. Greenwood, M. J. Hails, J. D. Kennedy, and W. S. McDonald, *J. Chem. Soc., Dalton Trans.*, 1981, 1415.
25 J. D. Kennedy and W. McFarlane, unpublished work.
26 (*a*) G. K. Barker, M. Green, F. G. A. Stone, and A. J. Welch, *J. Chem. Soc., Dalton Trans.*, 1980, 1186; (*b*) M. J. Calhorda, D. M. P. Mingos, and A. J. Welch, *J. Organomet. Chem.*, 1982, **228**, 309.
27 S. K. Boocock, N. N. Greenwood, and J. D. Kennedy, *J. Chem. Soc., Chem. Commun.*, 1980, 305.
28 T. B. Marder, R. T. Baker, J. A. Long, J. A. Doi, and M. F. Hawthorne, *J. Am. Chem. Soc.*, 1981, **103**, 2988.
29 W. F. Wright, A. R. Garber, and L. J. Todd, *J. Magn. Reson.*, 1978, **30**, 595.
30 (*a*) D. Reed, G. Ferguson, B. L. Ruhl, O. Ni Dhubhghaill, and T. R. Spalding, *Polyhedron*, 1988, **7**, 17; (*b*) G. Ferguson, M. J. Hampden-Smith, O. N. Dhubhghaill, and T. R. Spalding, *ibid.*, p. 187.

31 E. W. Corcoran and L. G. Sneddon, *J. Am. Chem. Soc.*, 1985, **107**, 7446.
32 G. B. Kauffman and D. O. Cowan, *Inorg. Synth.*, 1960, **6**, 211.
33 'International Tables for *X*-Ray Crystallography,' Kynoch Press, Birmingham, 1974, vol. 4.
34 B. Frenz and Associates Inc., College Station Texas 77840 and Enraf-Nonius, Delft, Holland, 1983.
35 C. K. Johnson, ORTEP II, Report ORNL-5138, Oak Ridge National Laboratory, Tennessee, 1976.
36 N. N. Greenwood, M. J. Hails, J. D. Kennedy, and W. S. McDonald, *J. Chem. Soc., Dalton Trans.*, 1985, 953.
37 X. L. R. Fontaine and J. D. Kennedy, *J. Chem. Soc., Dalton Trans.*, 1987, 1573.
38 M. Bown, X. L. R. Fontaine, and J. D. Kennedy, *J. Chem. Soc., Dalton Trans.*, 1988, 1467.
39 S. K. Boocock, N. N. Greenwood, J. D. Kennedy, W. S. McDonald, and J. Staves, *J. Chem. Soc., Dalton Trans.*, 1981, 2573.
40 X. L. R. Fontaine, H. Fowkes, N. N. Greenwood, J. D. Kennedy, and M. Thornton-Pett, *J. Chem. Soc., Dalton Trans.*, 1987, 1431, 2417.
41 M. Bown, X. L. R. Fontaine, N. N. Greenwood, J. D. Kennedy, and M. Thornton-Pett, *J. Chem. Soc., Dalton Trans.*, 1987, 1169.
42 J. D. Kennedy and J. Staves, *Z. Naturforsch., Teil B*, 1979, **34**, 808.
43 R. J. Goodfellow, in 'Group VIII transition metals,' ch. 20 in 'Multinuclear N.M.R.,' ed. J. Mason, Plenum, London, and New York, 1987, pp. 521—562.
44 W. McFarlane, *Proc. R. Soc. London, Ser. A*, 1968, **306**, 185.

Received 25th November 1987; Paper 7/2098